Improving Temporal Coverage of the SWOT Mission Using Spatiotemporal Kriging

Yeosang Yoon, Michael Durand, Carolyn J. Merry, and Ernesto Rodríguez

***Abstract*—The upcoming Surface Water and Ocean Topography (SWOT) satellite mission will measure water surface elevation, its spatial and temporal derivatives, and inundated area. These observations can be used to estimate river discharge at a global scale. SWOT will measure a given area on mid-latitude rivers two or three times per 22-day repeat cycle. In this paper, we suggest an interpolation-based method of estimating water height for times without SWOT observations (i.e., in between SWOT overpasses). A local space-time ordinary kriging (LSTOK) method is developed. Two sets of synthetic SWOT observations are generated by corrupting two different types of true river height with the instrument error. The true river heights are extracted from: 1) simulation of the LISFLOOD-FP hydrodynamic model, and from 2) in situ gage measurements from five USGS gages. Both of these synthetic SWOT observations datasets are important for the following reasons. The model-based dataset provides a complete spatiotemporal picture of river height that is unavailable from in situ measurements, but neglects the effects of e.g. human management actions on river dynamics. On the other hand, the gage-based dataset samples only five locations on the river (1,050 km in length), but represents all effects of human management, tributaries, or other influences on river heights, which are not included in the model. The results are evaluated by a comparison with truth and simple linear interpolation estimates as a first-guess. The model-based experiment shows the LSTOK recovered the river heights with a mean spatial and temporal root mean square error (RMSE) of 11 cm and 12 cm, respectively; these accuracies show a 46% and 54% improvement compared to the RMSEs of the linear interpolation estimates. The gage-based experiment shows a temporal RMSE of 32 cm on average; the LSTOK estimates show a 23% improvement over the linear interpolation estimates. The degradation in performance of the LSTOK for the gage-based analysis as compared to the model-based analysis is apparently due to the effects of human management on river dynamics. Further work is needed to model the effects of human management, and to extend the analysis to consider river tributaries and the main stem of the river simultaneously.**

***Index Terms*—Kriging, river height and discharge, SWOT, temporal resolution.**

Manuscript received October 15, 2012; revised February 01, 2013; accepted March 20, 2013. Date of publication April 30, 2013; date of current version June 17, 2013. This work was supported by NASA Headquarters under the NASA Earth and Space Science Fellowship Program-Grant NNX11AL60H, and the NASA Physical Oceanography grant NNX10AE96G. Computational support for this project was provided by the Ohio Supercomputer Center, under project PAS0503.

Y. Yoon and C. J. Merry are with the Department of Civil, Environmental, and Geodetic Engineering, The Ohio State University, Columbus, OH 43210 USA. They are also with the Byrd Polar Research Center, The Ohio State University, Columbus, OH 43210 USA (e-mail: yoon.203@osu.edu).

M. Durand is with the School of Earth Sciences, The Ohio State University, Columbus, OH 43210 USA. He is also with the Byrd Polar Research Center, The Ohio State University, Columbus, OH 43210 USA.

E. Rodríguez is with the Jet Propulsion Laboratory, California Institute of Technology, Pasadena, CA 91109 USA.

Color versions of one or more of the figures in this paper are available online at http://ieeexplore.ieee.org.

Digital Object Identifier 10.1109/JSTARS.2013.2257697

I. Introduction

SATELLITE remote sensing data have been utilized to provide spatial and temporal variations in terrestrial surface water heights [1]. In particular, satellite radar nadir altimetry (e.g., TOPEX/Poseidon, ERS-1/2, ENVISAT, and Jason-1/2 missions) has been shown to be successful when used for studying water surface elevation (WSE) [2], [3]. However, radar nadir altimetry provides only spot measurements of WSE instead of two-dimensional measurements of WSE. The upcoming Surface Water and Ocean Topography (SWOT) mission is a wide-swath altimeter, rather than a nadir altimeter providing point measurements [1], [4]. Thus, the SWOT mission will provide high-resolution images of inland WSE, as well as mapping of inundated extent and surface expression of storage changes. Over recent years, a number of studies have explored how to characterize river discharge and water storage changes using SWOT data [5]–[11].

The currently proposed 22-day SWOT orbit will provide full global coverage and will measure each point on the Earth's surface a minimum of twice per cycle. Specifically, for mid-latitude rivers, most areas are measured two or three times, and some areas are measured four times per 22-day cycle [8]. Thus, temporal sampling intervals of SWOT will be significantly better, compared to current satellite altimeters. Nonetheless, at a given location on a river, SWOT measurements will not be available on a daily frequency.

The goal of this study is to present a method of estimating the river height for times without SWOT observations (i.e., in between SWOT overpasses). In formulating our interpolation strategy, we exploit the nature of flood waves. Flood waves are translatory, in that they propagate downstream, creating at each location a similar disturbance in the water surface elevation [12]. Thus, a hydrologic event that is unobserved on one part of the river network is likely to be observed either downstream or upstream. Due to this fluvial interconnection, river hydraulic variables exhibit spatiotemporal correlation, a fact that has been exploited in past studies to interpolate hydraulic data on rivers [13]–[16]. Most flood waves are dynamic (rather than kinematic) in that typical flood waves are attenuated downstream due to the effects of friction [12]. Moreover, changes in channel width and bed slope downstream would be expected to modify the shape of the hydrograph. Our working hypothesis is that this change in shape in the nature of the flood wave downstream is predictable and can be modeled statistically using a relatively simple spatiotemporal correlation function. We suggest a space-time interpolation technique to accomplish our goal, implicitly considering the effects of floodwave

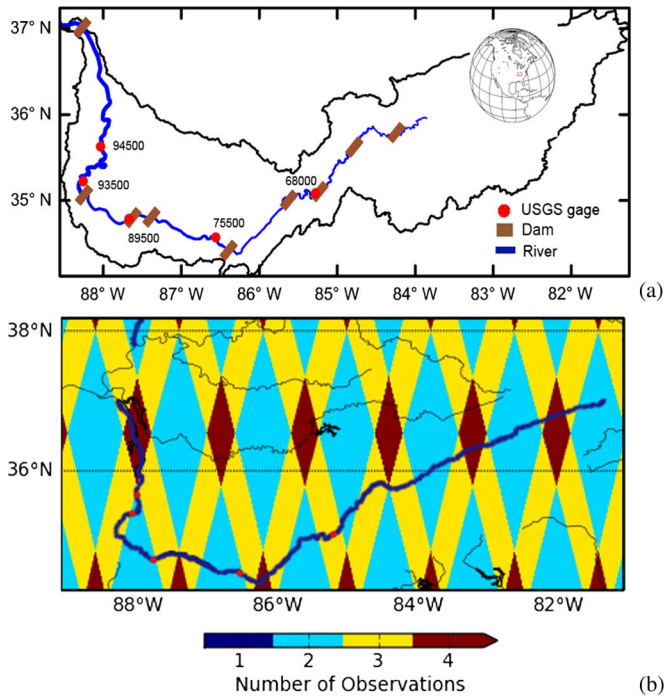

Fig. 1. A map of the Tennessee River Basin (a), showing the USGS gages (red dots) and dams (brown) used for this study. In order from upstream, the dams are: Fort Loudoun Dam, Watts Bar Dam, Chickamauga Dam, Nickajack Dam, Guntersville Dam, Wheeler Dam, Wilson Dam, Pickwick Landing Dam, and Kentucky Dam. The number of SWOT observations per 22-day cycle over the area is also shown (b).

attenuation and river channel geometry on flood wave propagation. We test and evaluate this approach using two different types of synthetic SWOT observations for the Tennessee River. One is simulated from modeled river heights using a hydrodynamic model and the other is generated from in situ gage measurements. The former dataset is more compatible with the SWOT spatial measurements, while the latter dataset includes the effects of un-modeled phenomena, such as lateral inflows and the effects of management on the river. We evaluate the results compared with truth datasets and linear interpolation estimates as a first-guess in terms of spatial and temporal accuracy. In addition, the performance of the two experiments are evaluated and discussed.

II. Study Area

This study focuses on the Tennessee River, the largest tributary to the Ohio River (Fig. 1). The Tennessee River is approximately 1,050 km long and drains an area of 105,000 km^2. The mean discharge is 2,000 m^3/s. The discharge is normally high in the winter season and is the lowest in September [17].

The main stem of the Tennessee River has nine dams/reservoirs used for hydroelectric power generation, flood control, and navigation (Fig. 1(a)). Those dams/reservoirs can be classified by two operating modes [18]. First is the storage mode to retain floodwater; seven reservoirs (Fort Loudoun Lake, Watts Bar Lake, Chickamauga Lake, Guntersville Lake, Wheeler Lake, Pickwick Lake, and Kentucky Lake) primarily operate in this mode. Second is the run-of-river mode to maintain a navigable water depth; two reservoirs (Nickajack Lake and Wilson Lake) primarily operate in this mode. Reservoir management decisions are based on current rainfall and runoff conditions, based on guide curves for each reservoir. Operating constraints, such as power generation, floods, and drought, also play a major role in decision-making. The red dots in Fig. 1(a) show the U.S. Geological Survey (USGS) stream gages (http://waterdata.usgs.gov) that were used for this study. The gages are located next to the Chickamauga Dam, Guntersville Dam, Wilson Dam, and Pickwick Landing Dam (in order of location from the upstream). For example, the Chickamauga Dam is located 758 km upstream from the mouth of the Tennessee River (just before gage 68000, Fig. 1(a)). The hydroelectric generation capacity is about 160 megawatts. The water elevation of the Chickamauga Reservoir is required to maintain at least 205.7 m in the summer and 207.9 m during the winter (elevations refer to meters above sea level). Flood control considerations are also highly important to the Tennessee Valley Authority (TVA) system of dams. The operation policy on flood risk varies from reservoir to reservoir, considering changes in peak flows and downstream flood conditions [18].

Clearly, if all of the reservoirs are operating under identical conditions and constraints, then one would expect the river heights downstream to maintain a high degree of correlation. However, if one reservoir operating rules differ from the others, or are subject to different operating conditions at certain times, then the flood waves will no longer propagate identically above and below the dams. The net effect of this is that the spatiotemporal autocorrelation of the water surface elevation will decrease due to the effect of human management. For example, consider the modeled and measured river height anomaly of gages 93500 and 94500 from days 0–100 shown in Fig. 2(b). These are the downstream-most gages. The modeled height anomalies are approximately constant during this time, with small variations of less than 1 m. The measured height anomalies for both gages decrease monotonically by approximately 1.5 m over the course of 100 days. Presumably, this water level decrease was driven by decreased releases from Pickwick Landing Dam.

III. Synthetic SWOT Observations

We generate two sets of the synthetic SWOT measurements by corrupting the two different types of true river height with the SWOT instrument error. Two different types of true river heights are used: the first is the modeled river height simulated by a hydrodynamic model, and the second is derived from USGS stream gage data. Each method has advantages and limitations. The hydrodynamic model can provide river heights of the entire study site, while the gage measurements are limited to the five gage locations. However, the modeled river heights may not sufficiently reflect the real system due to simplifying assumptions and un-modeled phenomena (e.g., lateral inflows, flood plains, and dams and reservoirs) in the hydrodynamic model, while all such factors are included in the gage measurements.

Interpolating synthetic SWOT measurements generated from a simplified hydrodynamic model (model-based SWOT), and using gaged heights on the same river (gage-based SWOT), should capture the two issues—simulation and truth—of how

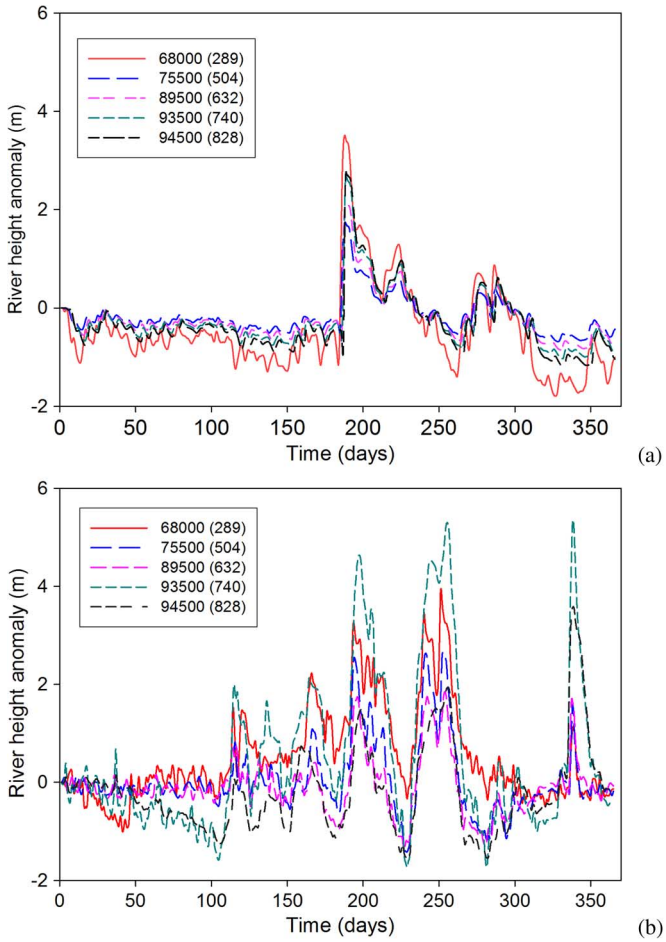

Fig. 2. Time series of SWOT water height anomaly generated from: (a) modeled water height (1991–1992), and (b) UGSG gaging water height (2009–2010). The numbers in parentheses refer to pixel location along the Tennessee River.

well the interpolation is expected to work. The simplified hydrodynamic model will not fully capture the true complex spatiotemporal correlations in a river; this model-based SWOT analysis is expected to represent an ideal case where we would expect interpolation to perform well. The Tennessee River is arguably a highly-regulated river system for hydroelectric power generation, flood control, and navigation, given the nine dams and reservoirs. Reservoirs and other human management actions may be expected to decrease the spatiotemporal autocorrelations between points on the river. The in situ gage measurements reflect not only human management actions, but also the river channel complexity (i.e., lateral inflows, floodplains, tributaries). In addition, as mentioned above, the lack of available gage measurements limits the sampling number for the gage-based SWOT analysis. Thus, we would expect interpolation of the gage-based SWOT to be a worst-case of how the interpolation would perform.

A. Virtual SWOT Observations Based on the Hydrodynamic Model

The generation of SWOT observations from the hydrodynamic model consists of three parts: generating a synthetic model-based "truth," modeling SWOT spatiotemporal sampling via orbit simulation, and modeling SWOT height error characteristics. First, the synthetic truths (e.g., river height, velocity, and discharge) are simulated by using the LISFLOOD-FP model. LISFLOOD-FP is a 1 D/2 D hydrodynamic model based on raster data input to represent floodplain flow and to simulate river channel flow using a rectangular channel approximation [19]. Here, we apply the 1 D scheme based on the diffusive wave approximation of the St. Venant equations to focus on hydrodynamic modeling of the in-channel flow [20]. For the LISFLOOD-FP model, the channel centerline, channel width, bed elevation, channel roughness, DEM, and upstream flow boundary conditions are needed. Here we use the model inputs described by Durand *et al.* [9]. The centerlines and bed elevations were derived from the Hydro 1 K dataset [21], which were defined at an approximately 1 km spatial resolution. The river channel widths are estimated from the Landsat-5 and Landsat-7 imagery [22] using the algorithm developed by Pavelsky and Smith [23]. The river depths and discharges extracted from the USGS gages were used as boundary conditions. The modeled time period is June 1, 1991 to May 31, 1992.

Second, the SWOT observations are simulated by overlaying the SWOT swath coverage on the synthetic truths. The SWOT swath coverage of 140 km is derived from the ground track that is simulated by using a predicted satellite location. The number of SWOT observations per 22-day cycle is shown in Fig. 1(b).

Third, the expected instrument errors are added to the synthetic truth data. In this study, we model only height measurement error. The instrument spatial resolution in the cross-track direction will vary from 70 m to 10 m; the best resolution in the along-track direction will be about 2 m. A more detailed specification of the SWOT mission is found in Rodríguez [24]. Here, we conservatively assume that the spatial resolution in both the along-track and cross-track directions is 50 m to simplify the measurement error model. The instrument measurement error is simulated with a zero mean Gaussian random error with a standard deviation of 50 cm for a 50 m by 50 m pixel, following previous work (e.g., [8], [9]). The resolution of the LISFLOOD-FP model and river widths used in the model are utilized to calculate a SWOT height error at each pixel, assuming that errors are uncorrelated in space to simplify the model. Based on these assumptions, we modeled height error standard deviations that range from 2.4 cm to 5.9 cm for a LISFLOOD-FP model pixel (1 km by 1 km).

B. Virtual SWOT Observations Based on In Situ Gage Data

Similar to the previous approach, we generated SWOT observations from in situ gage data by considering the SWOT swath coverage and sensor orbit sampling, as well as corrupting the observations with instrument error. Here, the time series of SWOT observations at only five locations of the study site is generated; the experimental period is June 1, 2009 to May 31, 2010. The main reason for the restricted datasets and time difference is the lack of available USGS gage measurements during other time periods; detailed information for the in situ gages used in the study is shown in Table I.

TABLE I
INFORMATION OF THE USGS GAGES USED TO DERIVE THE RIVER HEIGHT FOR GENERATING SYNTHETIC SWOT OBSERVATIONS

USGS gage ID	Flow distance from upstream (km)	SWOT revisit days per cycle
68000	289	4, 16, 19
75500	504	16, 22
89500	632	13, 19
93500	740	10, 16
94500	828	10, 16

Fig. 2 shows the time series of gage-based SWOT observations (in terms of height anomaly) for the Tennessee River, as well as the time series of model-based SWOT observations at the same gage locations; note that the experimental time periods are different for the model and gage-based analysis. The temporal profile between the model-based SWOT (Fig. 2(a)) and the gage-based SWOT (Fig. 2(b)) varies, even considering the differences of the selected experimental period. While the height anomaly of the model-based SWOT shows a fairly steady flow pattern, the height anomaly of gage-based SWOT shows an irregular flow pattern at certain time periods (see Fig. 2(b)). For example, the height ranges of gages 68000 and 77500 are significantly different at 4.8 m and 1.7 m, respectively. The height anomaly for gage 68000 shows a monotonically decreasing pattern during the first 50 days. The correlation coefficient between the gages 68000 and 77500 is -0.25. Presumably, the irregular gage records may reflect the activities of the Chickamauga Dam operation, such as for flood control or hydroelectric power generation. On the other hand, the river model for the Tennessee River did not consider locks and dams, which leads to differences of temporal patterns in the real situation and the modeled river depth.

IV. SPATIOTEMPORAL INTERPOLATION STRATEGY

We interpolate the SWOT river height anomaly instead of absolute river height to limit the differences of bed elevation between the stream locations. The river height anomaly Δh is estimated by subtracting the river height h from the initial river height $h(0)$ for an experimental period; note $\Delta h = h - h(0)$. We assume that $h(0)$ is known, but it can be replaced with the average river height, if an accumulation of SWOT observations becomes sufficient in the future.

In this study, we essentially adapt the temporal ordinary kriging (OK) approach by 1) calculating a time lag between pixels to allow for the flood wave travel time; and 2) allowing both the decorrelation time and the height anomaly variance to be different at each pair of pixels, which accounts for the effects of a spatially-variable river bed form on the temporal variations in water height. In sum, this amounts to a temporal ordinary kriging, adjusted by a spatially-dependent lag time, variance, and decorrelation time. Our approach is explained in more detail below.

A. Ordinary Kriging

OK is a geostatistical method with a goal to minimize the error variance. OK is suited to interpolate geo-hydrological variables from sparse observations (e.g., [13], [14]). Estimates of unobserved values $\hat{Z}(x_0)$ are calculated using weighted linear combinations of the available data:

$$\hat{Z}(x_0) = \sum_{i=1}^{n} \lambda_i Z(x_i) \tag{1}$$

where $Z(x_i)$ is the measured value at location i, and λ_i is the corresponding weight, which is estimated by specifying the autocorrelation function relating measurements of $Z(x_i)$ across space and time. To ensure that $\hat{Z}(x_0)$ is unbiased, the sum of the weights is constrained to unity:

$$\sum_{i=1}^{n} \lambda_i = 1. \tag{2}$$

In order to minimize the variance of the modeled error, the Lagrange parameters technique is utilized. A more detailed description for the OK method is founded in Isaaks and Srivastava [25].

B. Local Space-Time Ordinary Kriging

In this study, our goal is to evaluate a potential method of estimating river height at unobserved times (i.e., in between SWOT overpasses) by the interpolation of SWOT measurements. In formulating our interpolation strategy, we exploit the nature of flood waves. Flood waves are translatory, in that they propagate downstream, creating at each location a similar disturbance in the water surface elevation. Thus, a hydrologic event that is unobserved on a given part of the river network is likely to be observed either downstream or upstream. For example, the Tennessee River near gage 75500 in Table I is observed on days 16 and 22 within the 22-day SWOT repeat period, but is not measured on other days. However, its upstream or downstream gages (i.e., gages 68000, 89500, and 93500) are measured on days 4, 10, 13, and 19 during the SWOT orbital period. Measurements for the Tennessee River near gage 75500 can be complemented using the upstream or downstream observed information.

The OK method is a straightforward technique to interpolate variables in only the spatial or in only the temporal domain [15]. In this study, however, we need to consider both spatial and temporal dependence. For instance, Fig. 3 shows the potential sample locations (i.e., SWOT coverage for both ascending and descending passes on day 16) to estimate the river height of a target location (pixel 632) that is not measured by SWOT on day 16. Note that the coverage of the sample location will vary corresponding to which day SWOT provides an estimate at the location. It is clear that while the river heights are measured the same day, each SWOT measurement shows obviously different values along the river channel due to the river channel geometry and lateral inflows. The differences cannot be fully defined by only spatial or temporal dependence. Fig. 4 shows a time series of modeled river height anomaly at pixels 504 and 632, separated by 130 km; these pixels correspond to the locations of gages 75500 and 89500, respectively. While there is clearly a strong coherence between the two time series, Fig. 4 illustrates several differences between the time series. First, there is a time lag: events occur at the upstream gage on the order of one day earlier than on the downstream gage. Second, the height

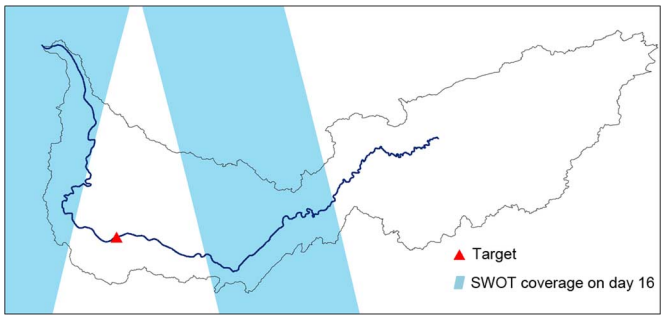

Fig. 3. Potential sample locations (i.e., SWOT coverage for both ascending and descending passes on day 16) for the target (pixel 632) that are not measured by the SWOT sensor on day 16.

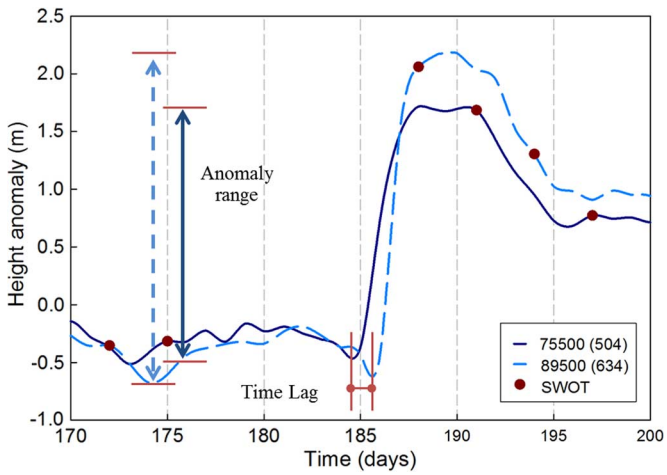

Fig. 4. Time series of river modeled river height anomaly at gages 75500 (pixel 504) and 89500 (pixel 632).

anomaly range at the downstream gage (3.0 m) is significantly greater than the height anomaly range at the upstream gage (2.3 m). The difference in range can be caused by the diffusion flood wave, lateral inflows, or channel geometry (e.g., bed slope and channel width) at the two locations. Our interpolation scheme must take these factors into account in order to be successful.

In this study, we utilize a local space-time ordinary kriging (LSTOK) method to address the variances of the river depth in the space and time domain, implicitly considering the effects of floodwave attenuation and river channel geometry on floodwave propagation. The primary analysis for the LSTOK scheme is identical to the OK method, interpolating from sparse observations based on optimal weights as shown in (1). The major difference between the OK and the LSTOK methods is the strategy for estimating the kriging weights λ. The weights of the OK method are traditionally generated from a semivariogram analysis, utilizing only spatial or only temporal dependence. On the other hand, the weights of the LSTOK are estimated to consider spatiotemporal phenomena. Our method proceeds as follows. First, we parameterize the covariance matrix. Specifically, for each pair of points, we parameterize three unknown variables in the variogram: the covariance between the time series σ^2, the lag between the time series Δt, and the de-correlation time τ between any two locations i and j in the study site. This amounts to

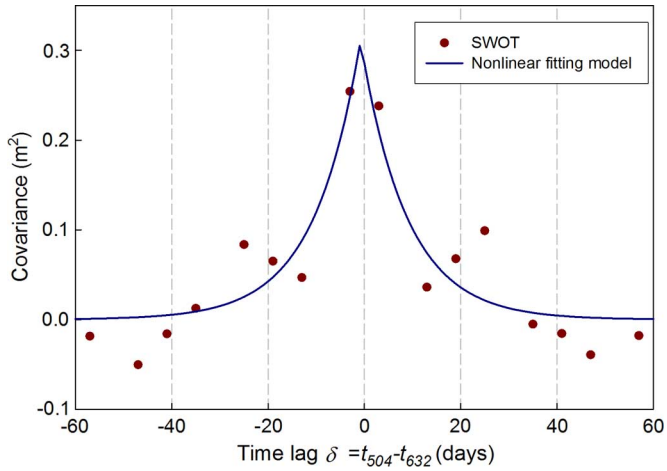

Fig. 5. Example result of nonlinear regression model used between pixels 504 and 632.

a modified semivariogram analysis, where we take into account the spatial dependence in height anomaly, as discussed above. Here, we first calculated the covariance $C_{i,j}(\delta = t_i - t_j; t$ is the vector of observation day of SWOT) between any two sample locations using a time series of synthetic SWOT measurements. Given the covariance, the variables are estimated using a nonlinear regression model; the nonlinear model is developed based on the Levenberg-Marquardt algorithm, which is an iterative technique to solve nonlinear least-squares problems [26]. We assume a modified exponential covariance model $M(i,j)$ between each pair of pixels in the domain:

$$M(i,j) = \sigma^2(i,j)\exp\left(\frac{-|\delta(i,j)+\Delta t(i,j)|}{\tau(i,j)}\right). \quad (3)$$

Fig. 5 shows an example result of the nonlinear fitting for three unknown variables between locations 504 and 632 from the model-based SWOT (previously shown in Fig. 4). From the nonlinear model, $\sigma^2(504,632)$, $\Delta t(504,632)$, and $\tau(504,632)$ are estimated as 0.33 m^2, 0.5 days, and 11.5 days, respectively.

Second, given the estimated $\sigma(i,j)$, $\Delta t(i,j)$, and $\tau(i,j)$ variables between any two locations i and j in the study site, we recalculate the spatiotemporal covariance between pairs of sample points, $c(i,j)$ using the modified exponential covariance model, as well as the spatiotemporal covariance between the sample points and the estimation point, $b(i,0)$.

$$c_{ij} = \sigma^2(i,j)\exp\left(\frac{-|\delta(i,j)+\Delta t(i,j)|}{\tau(i,j)}\right) \quad (4)$$

$$b_{i0} = \sigma^2(i,0)\exp\left(\frac{-|\delta(i,0)+\Delta t(i,0)|}{\tau(i,0)}\right) \quad (5)$$

Finally, the weight matrix of the LSTOK is defined as:

$$w = \tilde{C}^{-1}D \quad (6)$$

where the weight matrix w contains each weight $\tilde{\lambda}$ of the unknown observations, and a Lagrange multiplier μ:

$$w = [\tilde{\lambda}_1 \ldots \tilde{\lambda}_n \mu]^T \quad (7)$$

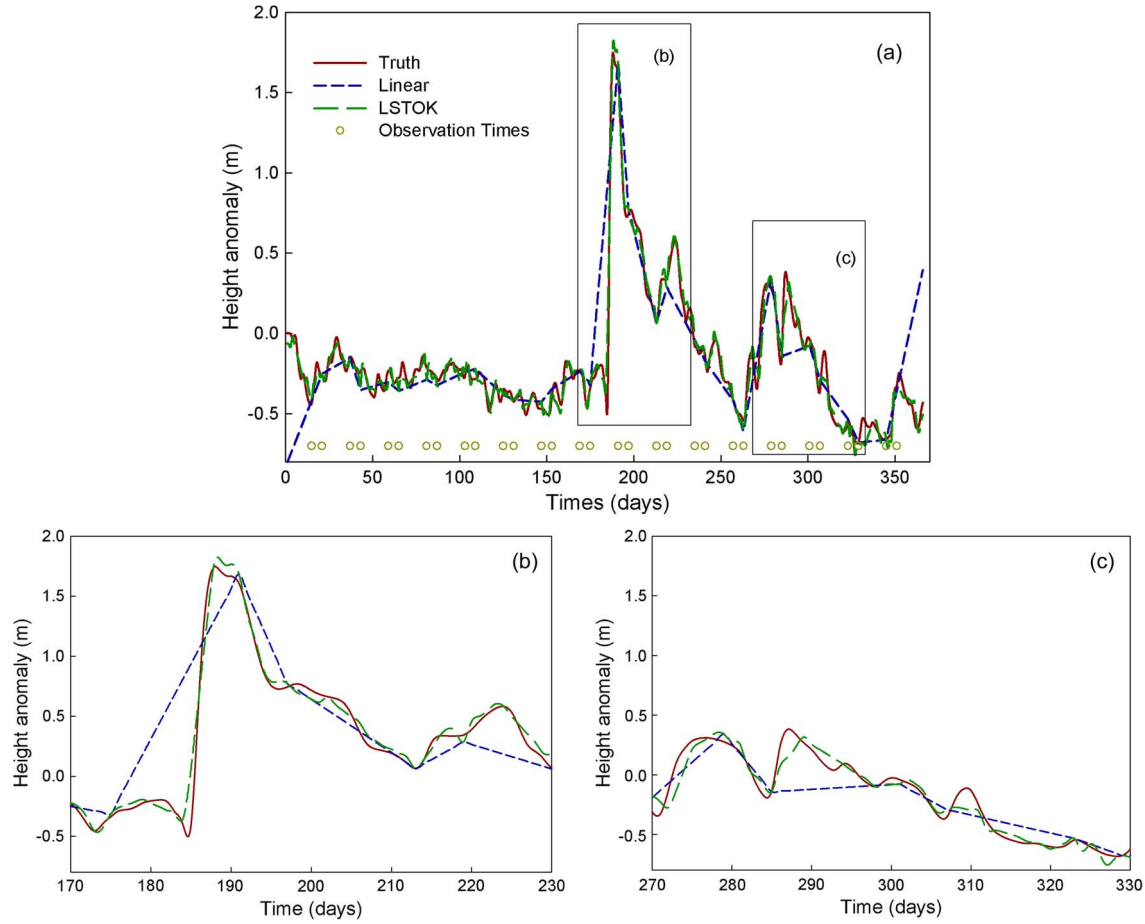

Fig. 6. Example of the estimates of the river height anomaly at pixel 504; the enlarged boxes—(b) and (c)—are shown for detail.

The matrix $\tilde{C}$ contains combinations of the spatiotemporal covariance c; the subscript n denotes the total number of observations:

$$\tilde{C} = \begin{bmatrix} c_{11} & \cdots & c_{1n} & 1 \\ \vdots & \ddots & \vdots & \vdots \\ c_{n1} & \cdots & c_{nn} & 1 \\ 1 & \cdots & 1 & 0 \end{bmatrix} \tag{8}$$

The matrix D contains a combination of the spatiotemporal covariance b:

$$D = [b_{10} \ldots b_{n0}\ 1]^T. \tag{9}$$

In addition, the LSTOK method contains a localization technique to reduce the computational burden of a covariance matrix. Observations located far from a given pixel do not include useful information for interpolation. For the localization scheme, we utilize a moving window technique with the search distance of 250 km, which is the range of spatial correlation that was found in our semivariogram analysis above.

C. Experimental Design

Observing system simulating experiments (OSSE) was designed for evaluating the potential for estimating river height for times without SWOT observations. The OSSE is a well-known technique to evaluate the potential impacts of new observing systems under consideration for deployment [5], [8]. Here, we present two experiments in the Tennessee River to evaluate the algorithm using two different types of SWOT observations, i.e., model-based SWOT (described in Section III-A) and gage-based SWOT (described in Section III-B). First, two different sets of truth river heights over the study site are extracted from the river modeling result and in situ gage data, respectively. Second, synthetic SWOT observations are generated from the truth river heights with instrument errors as described in Section III. Third, river heights for times without SWOT observations are estimated using the LSTOK method described in Section IV. Finally, the results are evaluated by a comparison with the true river heights. Linear interpolation is the simplest method to make an inference on missing values. Here, we used the simple linear interpolation method as a first-guess to fill the temporal gap of the SWOT observations. In addition, we evaluate and discuss the performance of the results from the two experiments.

V. Results and Discussion

A. Model-Based SWOT Observations

Fig. 6 shows the example LSTOK estimates of river height anomaly at the location around 504 km from the upstream location, compared with the truth and linear interpolation estimates. The linear interpolation estimates of height anomaly at

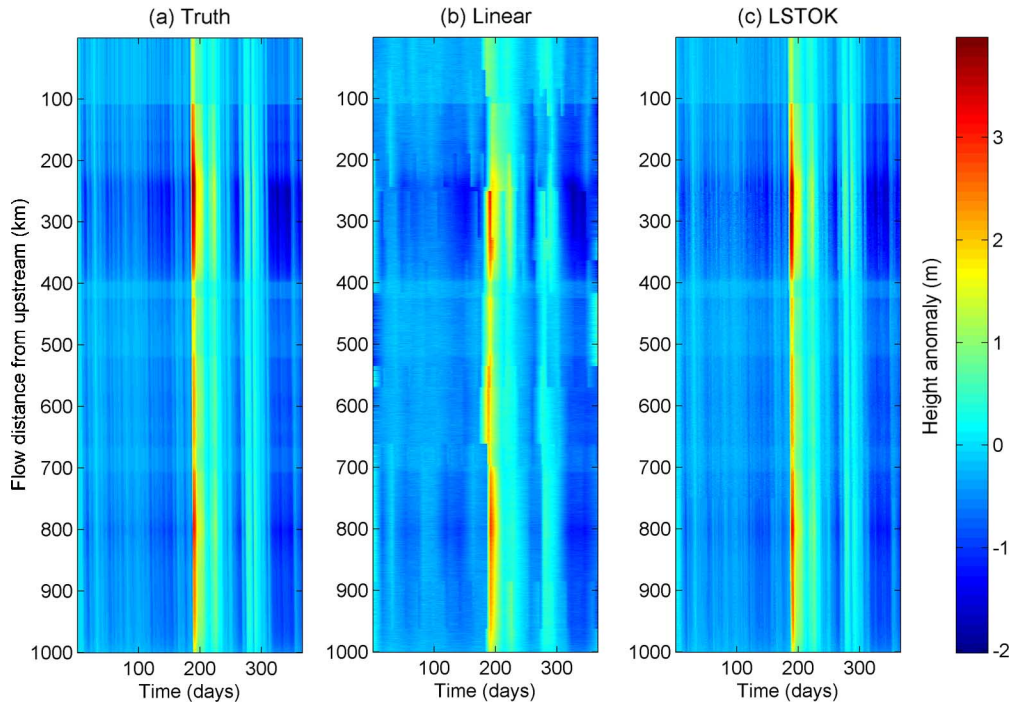

Fig. 7. River height anomaly along the river channel vs. time for (a) truth, (b) linear interpolation estimates, and (c) LSTOK estimates.

TABLE II
MEAN TEMPORAL RMSE OF RIVER DEPTH ANOMALY BETWEEN THE TRUTH, AND LINEAR INTERPOLATION AND LSTOK FROM GAGE-BASED SYNTHETIC SWOT OBSERVATIONS. THE IMPROVEMENT IN THE LSTOK METHOD COMPARED TO THE LINEAR INTERPOLATION IS ALSO SHOWN

USGS gage ID	Linear (RMSE, cm)	LSTOK (RMSE, cm)	Improvement
68000	36	30	17%
75500	38	27	30%
89500	32	23	28%
93500	65	50	23%
94500	37	31	17%
Mean	42	32	**23%**

this location had a 24 cm root mean square error (RMSE). While the estimates do miss some abrupt changes in river height, the LSTOK estimates of height anomaly are clearly improved over the linear interpolation estimates. The LSTOK error shows a 7 cm RMSE, which is a 72% improvement over the linear interpolation estimates. Note that the interpolation is applied to noisy measurements with a standard error ranging from 2.4 to 5.9 cm (as discussed in Section III). Fig. 7 shows the time series of river height anomaly along the entire river channel for the truth, linear interpolation, and the LSTOK method. While both linear and LSTOK interpolations yield a spatiotemporal pattern similar to the truth, the linear interpolator generally has more rapid transitions in height for the major event occurring during the 190–200 day period. The linear interpolator also misses many transitions in flow (visible as vertical lines in the truth) during the low flow period in the first 150 days of the study period. Visually, the LSTOK estimate captures these variations much better.

Fig. 8 shows the time series of river height anomaly errors for the estimates compared to the true state. Although errors persist in the LSTOK height estimate during the major event from day 190–200, they are dramatically reduced, from maxima between −200 cm and 300 cm, with errors generally on the order of 20 cm to 30 cm. The LSTOK approach clearly leads to an improvement of the accuracy in both the space and time domain and shows the possibility to estimate river height at unobserved times. The mean spatial and temporal RMSEs of LSTOK estimates are 11 cm and 12 cm, respectively; the errors show a 46% and 54% improved accuracy compared to RMSEs of 20 cm and 25 cm for the linear interpolation estimates, respectively.

B. Gage-Based SWOT Observations

Fig. 9 shows the example LSTOK estimates of river height anomaly at gage 75500, compared with the truth and linear interpolation estimates. The linear interpolation estimates had 38 cm RMSE; the estimates clearly miss the abrupt changes of the river height. A visual inspection of Fig. 9 shows that the LSTOK estimates recover much of the temporal variations in height anomaly that were missed in the linear interpolation. The error of the LSTOK estimate is 27 cm, which is 30% less than the linear interpolation estimates.

Table II shows the mean temporal RMSE of each gage location in the Tennessee River, comparing the truth with the linear interpolation and LSTOK estimates. Overall, the LSTOK estimates show a 23% improvement in terms of temporal RMSE compared to the linear interpolation estimates; the improvements vary from 17% to 30%. The USGS gages 75500 and 89500 show more improvement than others. The reason for this is apparently that both are fairly highly correlated with the upstream-most gage 68000. This is due to the fact that gage 68000 is measured on three days, only one of which overlaps with either the 75500 or 89500 gages (see Table I). The measurement at 68000 on day 4 is likely very important, in this regard. Note

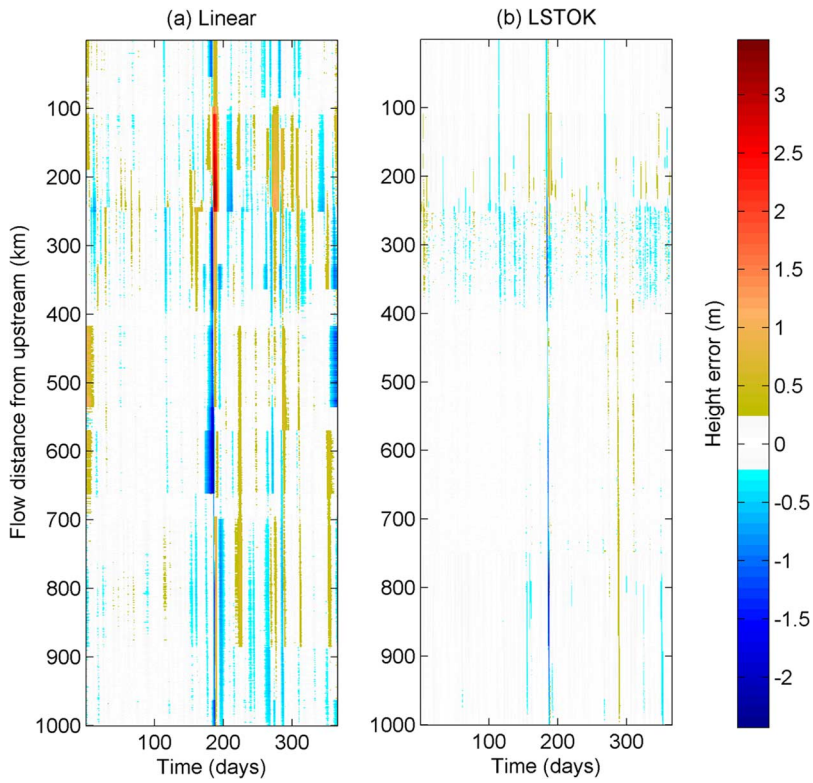

Fig. 8. Errors of river height anomaly along the river channel vs. time for (a) linear interpolation estimates, and (b) LSTOK estimates.

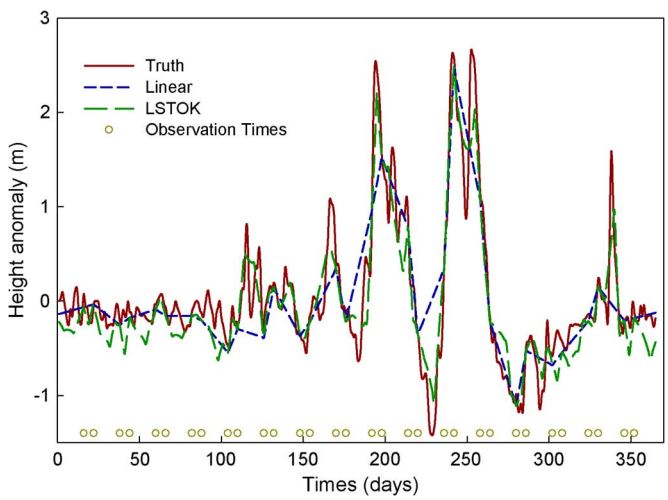

Fig. 9. The height anomaly estimates at gage 75500 using the gaged-based SWOT observations.

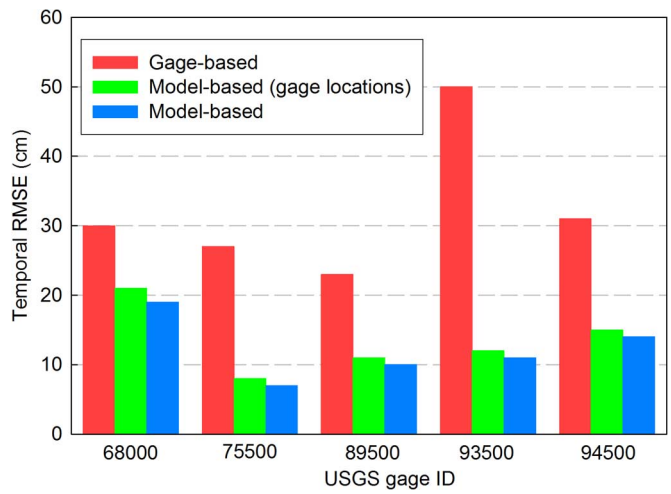

Fig. 10. The temporal RMSE for the five gages (the gage-based analysis, model-based analysis using the five gage location datasets, and the model-based analysis based on the entire datasets).

that at gage 75500, there is a 16-day gap between the measurements on day 22 for a given cycle, and that on day 16 of the next cycle. There is another 16-day gap at 89500, as well. The measurement on day 4 significantly reduces the size of the measurement gap, highlighting the utility of the LSTOK interpolator. Measurements at other gages also help reduce the size of the measurement gap. In the case of gage 68000, the size of the measurement gap can be reduced from measurements at gages 75500 and 89500. However, gage 68000 shows less correlation to gages 75500 and 89500, with a 17% improvement, which is the lowest improvement compared to all the gages. The downstream gages 93500 and 94500 are located at 451 km and 539 km, respectively, from gage 68000; thus, the day 4 measurements are less useful to the downstream gages. In addition, gages 93500 and 94500 are highly correlated between themselves and are observed at the same time, which reduces the performance of the LSTOK method.

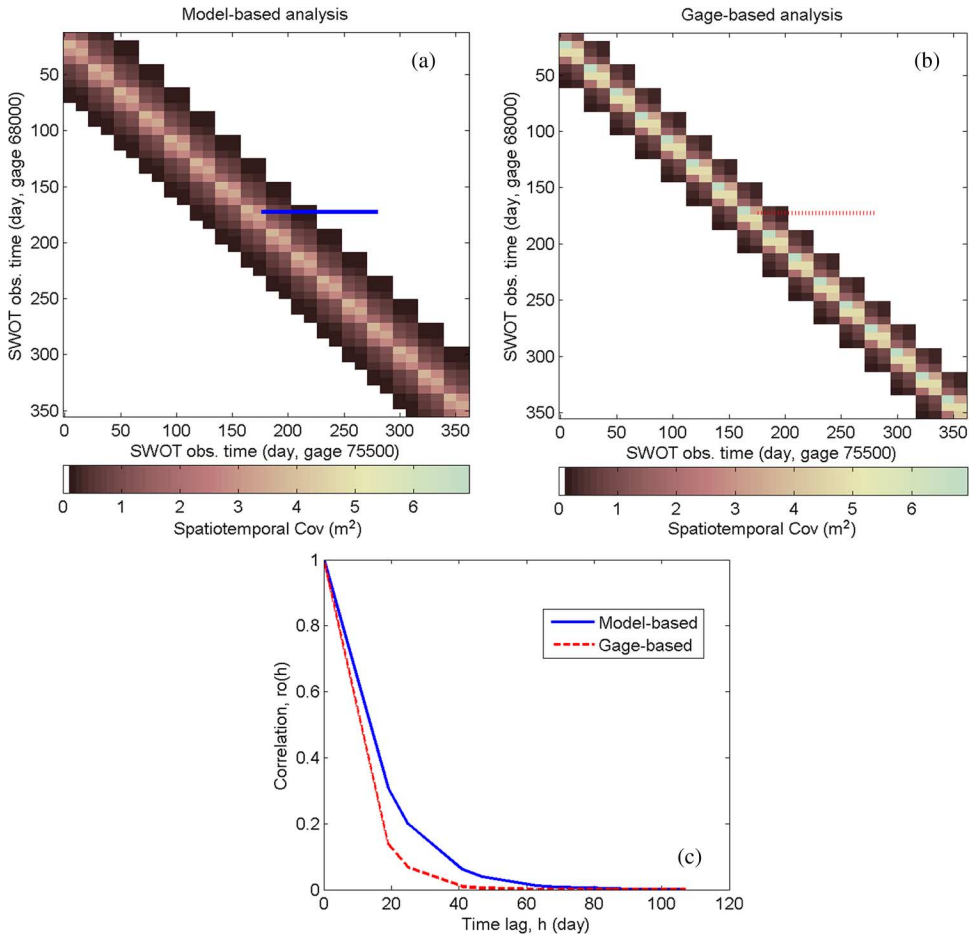

Fig. 11. Spatiotemporal covariance matrix between gages 68000 (pixel 289) and 75500 (pixel 504), for (a) model-based analysis, and (b) gage-based analysis. The horizontal line in figures (a) and (b) refers to day 173 of the SWOT observation. The correlation profile for day 173 is shown in (c).

C. On the Difference Between the Model-Based and Gage-Based Analysis

The analysis thus far shows that the LSTOK method showed a 54% improvement over the linear interpolator for the model-based SWOT analysis, and a 23% improvement over the linear interpolator for the gage-based SWOT analysis. The reason for the difference is two-fold. First, the river itself is likely to exhibit less correlation in reality than in the model. One of the major reasons is that human decisions govern whether water is released from a dam or not (refer to the location of gages in Fig. 1(a)). The existence of dams and reservoirs along the river channel can also decrease the correlation. This would be difficult or impossible to model using a parsimonious autocorrelation function. Indeed, the positive results shown in Fig. 9 indicate that at least for this river, human control of the river does not completely deteriorate the spatiotemporal autocorrelation in river height anomaly. The second reason for the difference between the gage and model analysis is that in the model-based SWOT case, there are 1,042 pixels measured, whereas there are only five gages. This large number of pixels means that there are measurements from more overpasses incorporated into the analysis. Incorporating even just one more overpass into the analysis made a significant difference in the gage-based analysis, as discussed in Section V-B. Note, too that the study periods are different for the model- and gage-based analysis (see Fig. 2), although this should not dramatically affect the difference between model- and gage-based analysis.

An important question is whether the effects of human control or the number of gage measurements is more important in the gage-based SWOT analysis not performing as well as the model-based SWOT. We can address this in part by redoing the model-based SWOT analysis, but only at the five pixels where we have gages. The SWOT observations, derived from the model-based SWOT, have the same number of observations and observing locations as the gage-based SWOT. Fig. 10 shows the temporal RMSE for the model-based SWOT, the gage-based SWOT, and the model-based SWOT at the gage locations. For all five gages, the RMSE of the model-based SWOT (using all 1,042 pixels) is very similar to the RMSE of the model-based SWOT based on the five gage locations. For instance, at gage 68000, the model-based SWOT RMSE (based on all 1,042 pixels) is 19 cm, and the model-based SWOT (based on five pixels at the gage locations) is 21 cm. For that gage, the gage-based analysis gives an RMSE of 30 cm. This analysis seems to show that the effects of human management on the river are more important than the fact that the gage-based analysis is only based on five locations.

Finally, we compare the parameterized covariance matrix for the model-based and gage-based analysis. A major difference

between the model-based and gage-based analysis is the lag distance in temporal dependence. Fig. 11 shows the example spatiotemporal covariance matrix between gages 68000 and 77500. In Fig. 11, the gage-based analysis shows an abrupt decrease in covariance at larger lag distances, compared to the model-based analysis. The correlation profile of day 173 at lag distances is shown in Fig. 11(c), which clearly represents this relationship. This indicates that gage-based SWOT observations are less correlated than the model-based SWOT observations, which affects the performance of the method. This is almost certainly due to the effects of human management on the river heights.

As a final caveat, it should be noted that the total standard deviation of the gage-based river height anomaly at these five pixel locations ranges from 59 to 161 cm. The linear interpolator decreases the RMSE to between 32 to 65 cm. The LTSOK interpolator we have proposed further reduces this to between 23 and 50 cm, an average improvement of 23%. From our model-based analysis this can be further improved to 11 or 12 cm for un-managed rivers. Finally, we should note that the decorrelation time is expected to be a function of river size [27]. The Tennessee River drains an area of 105,000 km^2, and has a mean discharge is 2,000 m^3/s; smaller rivers may be expected to perform less well.

VI. Conclusions

In this study, we present a modified ordinary kriging method for interpolating river heights from the SWOT mission. The algorithm is evaluated using two different types of synthetic SWOT observations (i.e., model-based SWOT and gage-based SWOT). These observations are modeled over the study site using the LISFLOOD-FP hydrodynamic model and in situ gage measurements, respectively. Using the model-based SWOT observations, the time series of river heights are estimated with the mean spatial and temporal RMSEs of 11 cm and 12 cm, respectively. The errors show a 46% and 54% improved accuracy compared to the linear interpolation estimates, respectively. Regarding the gage-based SWOT observations, the river height estimates show a 23% improvement compared to the linear interpolation estimates. Based on a third experiment, it seems that the reason is the differences in spatiotemporal autocorrelation, due to the role of human management of the river.

Overall, these results suggest that the LSTOK method will prove useful for interpolating SWOT observations. The recovered time series of river height can lead to an improvement in estimation of river discharge via the Manning's equation (e.g., [9]) and may be used to anticipate a hydrologic event leading to better water resources management.

In this study, we develop and explore the LSTOK method using datasets of a single main channel. In the future, a complex river network with multiple tributaries and floodplains needs to be considered for use in general purpose applications. To address this, we may need to extend the method using, for example, a conditional simulation technique [28] that can give an advantage in the assumption of stationarity and variations of the mean value. Future work will also consider the generation of more realistic SWOT observations by adding additional type of errors, such as atmospheric and geometric effects. Beyond the SWOT observations, the much larger constellation of altimeters (e.g., JASON-1/2, Sentinel, Cryosat, etc.) will collectively provide point sampling, which will give additional benefits for the method. Future work will also investigate the feasibility of incorporating multi-sensor observations.

Acknowledgment

The authors would like to thank the four anonymous reviewers who provided helpful comments and improved the quality of the paper.

References

[1] D. E. Alsdorf, E. Rodríguez, and D. P. Lettenmaier, "Measuring surface water from space," *Rev. Geophys.*, vol. 45, no. 2, p. RG2002, 2007, 10.1029/2006RG000197.

[2] A. V. Kouraev, E. A. Zakharova, O. Samain, N. M. Mognard, and A. Cazenave, "Ob' river discharge from TOPEX/Poseidon satellite altimetry (1992–2002)," *Remote Sens. Environ.*, vol. 93, pp. 238–245, 2004.

[3] F. Papa, F. Durand, W. B. Rossow, A. Rahman, and S. K. Bala, "Satellite altimeter-derived monthly discharge of the Ganga-Brahmaputra River and its seasonal to interannual variations from 1993 to 2008," *J. Geophys. Res.*, vol. 115, p. C12013, 2010, 10.1029/2009JC006075.

[4] M. Durand, L. Fu, D. P. Lettenmaier, D. E. Alsdorf, E. Rodríguez, and D. Esteban-Fernandez, "The surface water and ocean topography mission: Observing terrestrial surface water and oceanic submesoscale eddies," *Proc. IEEE*, vol. 98, no. 5, pp. 766–779, 2010.

[5] K. M. Andreadis, E. A. Clark, D. P. Lettenmaier, and D. E. Alsdorf, "Prospects for river discharge and depth estimation through assimilation of swath-altimetry into a raster-based hydrodynamics model," *Geophys. Res. Lett.*, vol. 34, p. L10403, 2007, 10.1029/2007GL029721.

[6] M. Durand, K. M. Andreadis, D. E. Alsdorf, D. P. Lettenmaier, D. Moller, and M. D. Wilson, "Estimation of bathymetric depth and slope from data assimilation of swath altimetry into a hydrodynamic model," *Geophys. Res. Lett.*, vol. 35, p. L20401, 2008, 10.1029/2008GL034150.

[7] S. Biancamaria, M. Durand, K. M. Andreadis, P. D. Bates, A. Boone, N. M. Mognard, E. Rodríguez, D. E. Alsdorf, D. P. Lettenmaier, and E. A. Clark, "Assimilation of virtual wide swath altimetry to improve Arctic river modeling," *Remote Sens. Environ.*, vol. 115, pp. 373–381, 2011.

[8] Y. Yoon, M. Durand, C. J. Merry, E. A. Clark, K. M. Andreadis, and D. E. Alsdorf, "Estimating river bathymetry from data assimilation of synthetic SWOT measurements," *J. Hydrol.*, vol. 464–465, pp. 363–375, Sep. 2012, 10.1016/j.jhydrol.2012.07.028.

[9] M. Durand, E. Rodríguez, D. E. Alsdorf, and E. Trigg, "Estimating river depth from remote sensing swath interferometry measurements of river height, slope, and width," *IEEE J. Sel. Topics Appl. Earth Observ. Remote Sens.*, vol. 3, no. 1, pp. 20–31, Mar. 2010.

[10] F. Papa, S. B. Biancamaria, C. Lion, and W. B. Rossow, "Uncertainties in mean river discharge estimates associated with satellite altimeter temporal sampling intervals: A case study for the annual peak flow in the context of the future SWOT hydrology mission," *IEEE Geosci. Remote Sens. Lett.*, vol. 9, no. 4, pp. 569–573, Jul. 2012.

[11] H. Lee, M. Durand, H. C. Jung, D. Alsdorf, C. K. Shum, and Y. Sheng, "Characterization of surface water storage changes in Arctic lakes using simulated SWOT measurements," *Int. J. Remote Sens.*, vol. 31, no. 14, pp. 3931–3953, Apr. 2010.

[12] S. L. Dingman, "Unsteady flow," in *Fluvial Hydraulics*. Oxford, U.K.: Oxford Univ. Press, 2009, ch. 11.

[13] K. Chokmani and T. B. M. J. Ouarda, "Physiographic space-based kriging for regional flood frequency estimation at ungagued sites," *Water Resour. Res.*, vol. 40, p. W12514, 2004, 10.1029/2003WR002983.

[14] R. S. V. Teegavarapu, "Use of universal function approximation in variance-dependent surface interpolation method: An application in hydrology," *J. Hydrol.*, vol. 332, pp. 16–29, Jan. 2007.

[15] S. Rouhani and D. E. Myers, "Problems in space-time kriging of geohydrological data," *Math. Geol.*, vol. 22, no. 5, pp. 611–623, 1990.

[16] L. Clement and O. Thas, "Estimating and modeling spatio-temporal correlation structures for river monitoring networks," *J. Agr. Biol. Envir. St.*, vol. 12, no. 12, pp. 161–176, 2007, 10.1198/108571107X197977.

[17] A. C. Benke and C. E. Cushing, *Rivers of North America*. Burlington, MA, USA: Elsevier Academic Press, 2005, pp. 384–390.
[18] TVA, 2004, "Reservoir operations study—Final programmatic EIS," TVA Document ch. 2 [Online]. Available: http://www.tva.gov/environment/reports/ros_eis/chapter2.pdf
[19] P. D. Bates and A. P. J. De Roo, "A simple raster-based model for flood inundation simulation," *J. Hydrol.*, vol. 236, pp. 54–77, Sep. 2000.
[20] M. A. Trigg, M. D. Wilson, P. D. Bates, M. S. Horritt, D. E. Alsdorf, B. R. Forsberg, and M. C. Vega, "Amazon flood wave hydraulics," *J. Hydrol.*, vol. 374, pp. 92–1015, Jul. 2009.
[21] Hydro 1 K Document. [Online]. Available: http://webgis.wr.usgs.gov/globalgis/metadata_qr/metadata/hydro1k.htm
[22] National Land Cover Dataset 2001. [Online]. Available: http://www.epa.gov/mrlc/nlcd-2001.html
[23] T. M. Pavelsky and L. C. Smith, "RivWidth: A software tool for the calculation of river widths from remotely sensed imagery," *IEEE Geosci. Remote Sens. Lett.*, vol. 5, no. 1, pp. 70–73, Jan. 2004.
[24] E. Rodríguez, SWOT Science Requirements Document, JPL Document, Initial Release, 2009 [Online]. Available: http://swot.jpl.nasa.gov/files/SWOT_science_reqs_final.pdf
[25] E. H. Isaaks and R. M. Srivastava, *An Introduction to Applied Geostatistics*. Oxford, U.K.: Oxford Univ. Press, 1989, ch. 12.
[26] G. A. F. Seber and C. J. Wild, *Nonlinear Regression*. New York, NY, USA: Wiley Series in Probability and Mathematical Statistics, 1989, ch. 14.
[27] S. Biancamaria, K. Andreadis, M. Durand, E. A. Clark, E. Rodriguez, N. Mognard, D. E. Alsdorf, D. P. Lettenmaier, and Y. Oudin, "Preliminary characterization of SWOT hydrology error budget and global capabilities," *IEEE J. Sel. Topics Appl. Earth Observ. Remote Sens.*, vol. 3, no. 1, pp. 6–19, Mar. 2010.
[28] A. G. Journel, "Geostatistics for conditional simulation of ore bodies," *Econ. Geol.*, vol. 69, pp. 673–687, 1974.

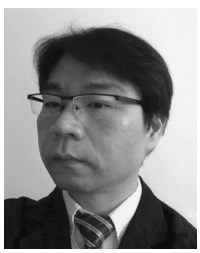

Yeosang Yoon received the B.E. and M.E. degrees in geodetic engineering from Inha University, Korea, in 1999 and 2001. He is currently completing the Ph.D. in civil engineering at The Ohio State University, Columbus, OH, USA.

His research interests include large-scale hydraulic and hydrologic modeling for monitoring impacts of climate change, land data assimilation for terrestrial water storage variation from satellite altimetry, and remote sensing techniques to environmental monitoring.

Michael Durand received the B.S. degree in mechanical engineering and biological systems engineering from Virginia Polytechnic Institute, Blacksburg, VA, USA, in 2002, and the M.S. and Ph.D. degrees in civil engineering from the University of California, Los Angeles, CA, USA, in 2004 and 2007, respectively.

He is currently an Assistant Professor with the School of Earth Sciences and the Byrd Polar Research Center, The Ohio State University, Columbus, OH, USA.

Carolyn J. Merry received the B.S. degree in geology from Edinboro University, Edinboro, PA, USA, the M.A. degree in geology from Dartmouth College, Hanover, NH, USA, and the Ph.D. degree in civil engineering from the University of Maryland, College Park, MD, USA.

She is Professor and Chair of the Department of Civil, Environmental and Geodetic Engineering at The Ohio State University (OSU), Columbus, OH, USA. Her current research projects include mapping water quality for Lake Erie using AVHRR, MODIS and SeaWiFS satellite data, and using Landsat-7 satellite data for mapping land cover change in the Lake Erie Watershed for use in biocomplexity modeling.

Ernesto Rodríguez received the Ph.D. degree in physics from the Georgia Institute of Technology, Atlanta, GA, USA, in 1984.

Since 1985, he has been with the Radar Science and Engineering Section, Jet Propulsion Laboratory, California Institute of Technology, Pasadena, CA, USA. His research interests include radar interferometry, altimetry, sounding, terrain classification, and EM scattering theory.